Formation of ZnO hexagonal micro-pyramids: a successful control of the exposed polar surfaces with the assistance of an ionic liquid†

Xi Zhou, Zhao-Xiong Xie,* Zhi-Yuan Jiang, Qin Kuang, Shu-Hong Zhang, Tao Xu, Rong-Bin Huang and Lan-Sun Zheng

Wurtzite ZnO hexagonal micro-pyramids, with all exposed surfaces being polar ± (0001) and {10$\bar{1}$1} planes, have been successfully synthesized using ionic liquids as solvents.

Anisotropy is a basic property of single crystals, and the various facets or directions in a crystal may exhibit different physical and chemical properties. Thus, surface architecture-controlled nanostructures are desirable for many applications.[1] For this purpose, the controllable preparation of micro/nanocrystals with different shapes and exposed surfaces is very important and challenging. Zinc oxide (ZnO), a wide band-gap semiconductor, plays an important role in many applications because of its extraordinary electrical and optical properties.[1–5] A variety of methods, ranging from template-assisted processes to vapor phase and solution phase syntheses, have been employed to fabricate ZnO nanostructures.[6] An effective way to achieve controlled growth is to apply the anisotropy of crystals, and has been demonstrated to be extremely successful in the synthesis of well shaped nanocrystals.[2,6b,7] For example, wurtzite ZnO usually tends to grow along the c-axis and maximizes the exposed areas of the {2$\bar{1}$$\bar{1}$0} and {01$\bar{1}$0} non-polar facets.[2] By either controlling the growth kinetics, doping, or through carbothermal reduction processes, it is possible to change the growth path of ZnO nanostructures.[8–11] Herein we demonstrate for the first time that in ionic liquid solvents, ZnO hexagonal micro-pyramids with all their exposed surfaces consisting of polar ± (0001) and {10$\bar{1}$1} planes can be easily synthesized. The key strategy is to vary the surface energy of the polar surfaces by strong electrostatic interactions between the ions of the ionic liquid and the polar surfaces. It is undoubted that this concept can be extended to the controlling of exposed surfaces and morphologies of a wide range of nanomaterials having similar structures.

Before showing the experimental results, we will firstly describe our strategy in detail. Structurally, the wurtzite-structured ZnO crystal is described as a number of alternating planes composed of four-fold tetrahedrally-coordinated O^{2-} and Zn^{2+} ions stacked alternatively along the c-axis.[12] The oppositely-charged ions produce positively-charged Zn (0001) and negatively-charged O (000$\bar{1}$) surfaces, resulting in a normal dipole moment and spontaneous polarization along the c-axis, as well as a divergence

in surface energy.[2] Besides the {0001} polar surfaces, ZnO has other typical polar surfaces: the {10$\bar{1}$1} surfaces.[6b,9] Interestingly, these polar surfaces make up hexagonal pyramids, as shown in the schematic model, Fig. 1A. In this model, the hexagonal pyramid consists of an O-terminated (000$\bar{1}$) surface for the base and O-terminated {10$\bar{1}$1} planes for the side surfaces, all of which are polar surfaces. We picture here the O-terminated surfaces because the O-terminated (000$\bar{1}$) polar surface is usually thought to be inert in comparison with the Zn-terminated ZnO (0001) polar surface.[12] The tip of the pyramid is along the [0001] direction, the Zn polarized direction. The calculated angle between two opposite edges at the tip of the pyramid is 63.94°, and the angle between the edge and the base plane is 58.03°.

During crystal growth, the polar surfaces usually appear as growing surfaces because of their high surface energy, and exhibit small facets or even disappear during the crystal growth. For example, in ZnO growth, the highest growth rate is usually along the c-axis and the large facets are usually {01$\bar{1}$0} and {2$\bar{1}$$\bar{1}$0} non-polar surfaces, rather than the polar {0001} surfaces. In contrast to the non-polar surfaces, the polar {10$\bar{1}$1} planes have a higher surface energy and usually grow too fast to be seen in the final shape of the crystal. As a result, polar surfaces are generally energetically unfavorable to be the exposed surfaces. To tune the
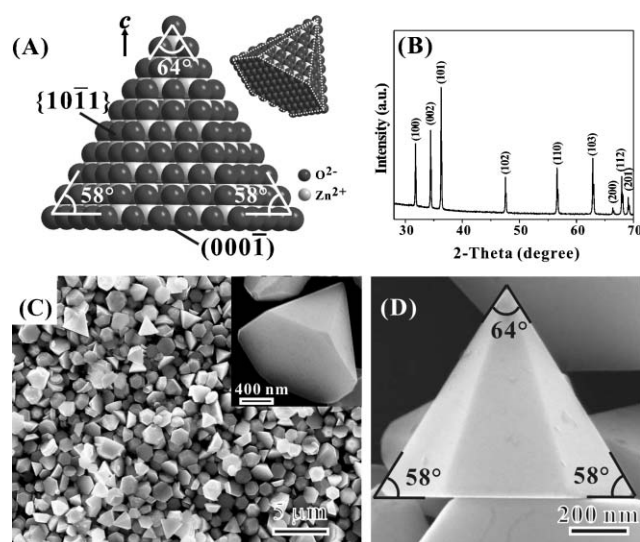

Fig. 1 (A) Schematic model of a ZnO hexagonal micro-pyramid, (B) XRD pattern of the as-prepared products, (C) SEM image of the morphology of the as-prepared products and an enlarged SEM image (inset), (D) SEM image of an individual ZnO hexagonal micro-pyramid.

State Key Laboratory for Physical Chemistry of Solid Surfaces and Department of Chemistry, College of Chemistry and Chemical Engineering, Xiamen University, Xiamen, 361005, China.
E-mail: zxxie@xmu.edu.cn; Fax: +86 592 2183047
† Electronic Supplementary Information (ESI) available: Experimental details, SEM images of ZnO products in different experimental conditions and TEM images of incomplete ZnO hexagonal pyramids. See DOI: 10.1039/b510287a

growth behavior of ZnO nanostructures, changing the surface energy should be effective. For example, the surface energy of the polar planes can be reduced by compensating the surface charge with a passivating reagent such as an ionic liquid. Due to the strong electrostatic interactions between the ions of the ionic liquid and the polar surfaces, the surface energies of the basal polar {0001} planes and the polar {10$\bar{1}$1} planes may decrease greatly in comparison to those of other crystal faces, resulting in a relatively slow growth rate for these polar planes. Thus the {0001} and {10$\bar{1}$1} planes may appear as exposed surfaces, as in the hexagonal pyramid structure.

Based on this strategy, ionic liquids should be effective in controlling the exposed facets. We chose a mixture of fatty acid (such as oleic acid (OA)) and organic amine (such as ethylenediamine) as the solvent, which can be thought as one kind of ionic liquid (R–COOH + R–NH$_2$ → R–COO$^-$ + R–NH$_3^+$). In a typical process, a mixture of OA and ethylenediamine (or trioctylamine, or methylamine) was used as the solvent (the growth environment), a similar method to which has been applied for the synthesis of ZnO quantum rods.[13] 6.6 ml OA and 4.5 ml ethylenediamine were mixed to give an orange liquid at room temperature. Then, 1.46 g anhydrous zinc acetate (Zn(CO$_2$CH$_3$)$_2$) was added. The resulting mixture was rapidly heated to 286 °C in 10–15 min and kept at 286 °C for 1 h. After reaction, the precipitates were collected and washed several times with hexane and ethanol. The final product was dispersed in ethanol for further characterization.

Fig. 1B shows an X-ray diffraction (XRD, PANalytical X-Pert diffractometer with Cu-Kα radiation) pattern of the as-prepared product taken from the OA and ethylenediamine solvent mixture. The diffraction peaks can be indexed as the wurtzite structure of ZnO (JCPDS 36-1451), indicating that the zinc acetate has been thermally decomposed into ZnO.[13] The scanning electron microscopy (SEM, LEO 1530) images display the general morphology of the as-prepared ZnO products (Fig. 1C), showing that the most striking feature of the product is the hexagonal micro-pyramids produced in very high yield (over 95%). In the Electronic Supplementary Information (ESI†), ZnO hexagonal micro-pyramids prepared from mixtures of OA and various amines are shown. The base size and the height of the ZnO hexagonal micro-pyramids are in the range of 1–1.5 μm. The six side surfaces and the base of the hexagonal micro-pyramids are very smooth. The angle between two opposite edges at the tip of the micro-pyramid is 64 ± 1°, and those between the base of the micro-pyramid and side edges are 58 ± 1°, as shown in Fig. 1D. This result implies that the micro-pyramids take the same structure as the proposed ZnO hexagonal pyramid model.

The intrinsic crystal structures of the hexagonal micro-pyramids were further investigated by high resolution transmission electron microscopy (HRTEM, FEI Tecnai-F 30 FEG), as shown in Fig. 2. The HRTEM image recorded (Fig. 2B) at the tip of a hexagonal micro-pyramid (Fig. 2A) shows the lattice spacing of 0.26 nm, corresponding to the distance between two (0002) crystal planes of wurtzite ZnO. Therefore, the base of the ZnO hexagonal micro-pyramid is the {0001} plane. The selected area electron diffraction (SAED) pattern further proves the hexagonal micro-pyramid to be a single crystal, with the pyramidal tip direction being along [0001] (Fig. 2C). To determine the polarity of the surfaces, the technique of convergent beam electron diffraction (CBED) was used.[14–17] Fig. 2D shows a CBED pattern recorded from the tip of the
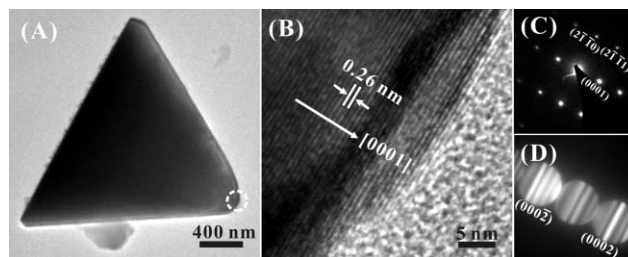

Fig. 2 (A) TEM image of an individual ZnO hexagonal micro-pyramid, (B) HRTEM image at the tip area marked in (A), (C) SAED pattern and (D) CBED pattern observed for the same ZnO micro-pyramid.

hexagonal micro-pyramid along the [01$\bar{1}$0] zone axis. Highly asymmetric (0002) and (000$\bar{2}$) diffraction discs for the wurtzite structure were observed.[18,19] The CBED result reveals that the tip of the hexagonal micro-pyramid is in the [0001] direction with Zn polarity, because the center of the diffraction disc appears bright in the right-hand spot.[14] As a result, the surface of the pyramidal base is the O-terminated (000$\bar{1}$) surface and the tip is the (0001) surface.

According to the above structure information, we may conclude that we have successfully synthesized ZnO micro-pyramids with polar lattice planes as exposed surfaces. The surface of the pyramidal base is an O^{2-}-terminated (000$\bar{1}$) plane, and the side surfaces are {10$\bar{1}$1} planes that are very possibly also O^{2-}-terminated. The SAED pattern from a truncated ZnO micro-pyramid supports {10$\bar{1}$1} as side surfaces.†

To demonstrate that ions in the mixtures of OA and organic amines play a key role in the formation of the polar surface-terminated pyramids, the thermal decomposition of zinc acetate in the air, pure OA and pure trioctylamine (TOA) was carried out. We did not choose pure ethylenediamine or methylamine as solvent for the thermal decomposition of zinc acetate because their boiling points are too low. As shown in Fig. 3, ZnO products from the pure OA were of irregular morphology, while nanorods were grown from either the air or TOA environments. Nanorods of both products take the <0001> as the longitudinal direction, which is the normal growth direction. The results show that only in the ionic liquid solvent (such as the mixture of OA and
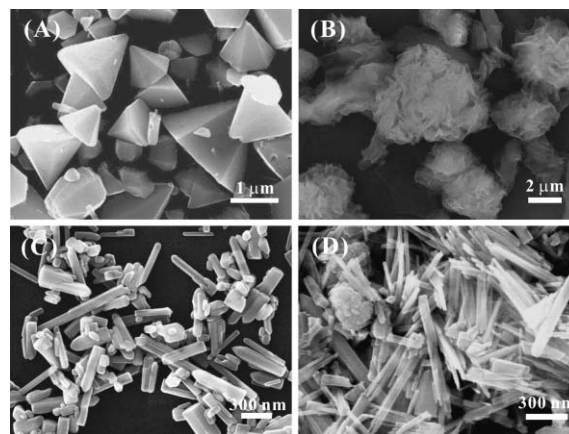

Fig. 3 SEM images of ZnO products prepared by thermal decomposition of zinc acetate in (A) a mixture of OA and TOA, (B) pure OA, (C) pure TOA (D) air.
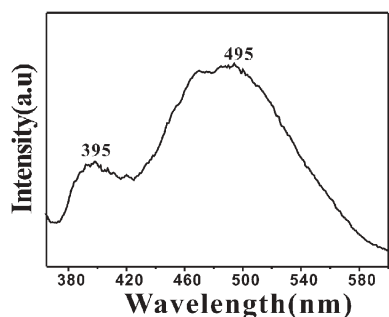
Fig. 4 The photoluminescence (PL) spectrum of as-prepared ZnO hexagonal micro-pyramids.

ethylenediamine) can the ZnO hexagonal micro-pyramids be grown.

Fig. 4 shows the photoluminescence (PL) spectrum of ZnO hexagonal micro-pyramids. A weak peak around 395 nm and a strong broad peak at 495 nm are observed in all the products, which correspond to the UV emission and green emission, respectively. The UV emission corresponds to the near band-edge emission of the wide band-gap ZnO, and the green band emission is thought to be related to intrinsic defect structures, in particular, oxygen vacancies originated from the oxygen deficiency.[20–22] A recent study shows that the green emission also originates from surface defects.[23] In the present case, the ZnO micro-pyramids were synthesized in an environment of ionic liquid. The surfaces of the micro-pyramids adsorb ions during their growth. It is reasonable to believe kinds of defect exist in the micro-pyramids, especially on their surfaces, and therefore strong green light emission from them is observed.

In conclusion, using ionic liquids as solvents, we have demonstrated a thermal decomposition synthesis of ZnO hexagonal micro-pyramids whose surfaces are enclosed by polarized $(000\bar{1})$ and $\{10\bar{1}1\}$ planes. The growth mechanism of the hexagonal micro-pyramid is due to ionic liquids lowering the surface energy of the polar surfaces. The technique demonstrated here can be extended for synthesizing a wide range of nanomaterials having similar structures.

Notes and references

1 *Nanowires and Nanobelts: Materials, Properties and Devices*, ed. Z. L. Wang, Tsinghua University Press, Beijing, 2004, vol. I and II.
2 Z. L. Wang, *J. Phys.: Condens. Matter*, 2004, **16**, R829.
3 Z. L. Wang, *Mater. Today*, 2004, **7**, 26.
4 Z. L. Wang, *Annu. Rev. Phys. Chem.*, 2004, **55**, 159.
5 M. H. Huang, S. Mao, H. Feick, H. Q. Yan, Y. Y. Wu, H. Kind, E. Weber, R. Russo and P. D. Yang, *Science*, 2001, **292**, 5523.
6 (*a*) Y. Li, G. W. Meng, L. D. Zhang and F. Phillipp, *Appl. Phys. Lett.*, 2000, **76**, 2011; (*b*) Z. L. Wang, X. Y. Kong, Y. Ding, P. X. Gao, W. L. Hughes, R. S. Yang and Y. Zhang, *Adv. Funct. Mater.*, 2004, **14**, 943; (*c*) Z. Y. Jiang, Z. X. Xie, X. H. Zhang, S. C. Lin, T. Xu, S. Y. Xie, R. B. Huang and L. S. Zheng, *Adv. Mater.*, 2004, **16**, 904; (*d*) J. Zhang, L. D. Sun, C. S. Liao and C. H. Yan, *Chem. Commun.*, 2002, **3**, 262.
7 L. Manna, E. C. Scher and A. P. Alivisatos, *J. Am. Chem. Soc.*, 2000, **122**, 12700; L. Manna, D. J. Milliron, A. Meisel, E. C. Scher and A. P. Alivisatos, *Nat. Mater.*, 2003, **2**, 382; L. Vayssieres, A. P. K. Keis, S. Lindquist and A. Hagfeldt, *J. Phys. Chem. B.*, 2001, **105**, 3350; J. T. Hu, T. W. Odom and C. M. Lieber, *Acc. Chem. Res.*, 1999, **32**, 435; M. Law, J. Goldberger and P. Yang, *Annu. Rev. Mater. Sci.*, 2004, **34**, 83.
8 X. Y. Kong and Z. L. Wang, *Nano Lett.*, 2003, **3**, 1625.
9 R. S. Yang, Y. Ding and Z. L. Wang, *Nano Lett.*, 2004, **4**, 1309.
10 X. S. Fang, C. H. Ye, L. D. Zhang, Y. Li and Z. D. Xiao, *Chem. Lett.*, 2005, **34**, 436.
11 X. H. Kong, X. M. Sun and Y. D. Li, *Chem. Lett.*, 2003, **32**, 546.
12 Z. L. Wang, X. Y. Kong and J. M. Zuo, *Phys. Rev. Lett.*, 2003, **91**, 185502.
13 M. Yin, Y. Gu, I. L. Kuskovsky, T. Andelman, Y. Zhu, G. F. Neumark and S. O'Brien, *J. Am. Chem. Soc.*, 2004, **126**, 6206.
14 K. Zou, X. Y. Qi, X. F. Duan, S. M. Zhou and X. H. Zhang, *Appl. Phys. Lett.*, 2005, **86**, 013103.
15 T. Mitate, Y. Sonoda and N. Kuwano, *Phys. Status Solidi A*, 2002, **192**, 383.
16 J. B. Baxter, F. Wu and E. S. Aydil, *Appl. Phys. Lett.*, 2003, **83**, 3797.
17 H. Kato, K. Miyamoto, M. Sano and T. Yao, *Appl. Phys. Lett.*, 2004, **84**, 4562.
18 B. Daudin, J. L. Rouviere and M. Arlery, *Appl. Phys. Lett.*, 1996, **69**, 2480.
19 F. Vigue, P. Vennegues, S. Vezian, M. Laugt and J. P. Faurie, *Appl. Phys. Lett.*, 2001, **79**, 194.
20 X. H. Zhang, S. Y. Xie, Z. Y. Jiang, Z. X. Xie, R. B. Huang, L. S. Zheng, J. Y. Kang and T. Sekiguchi, *J. Solid State Chem.*, 2003, **173**, 109.
21 M. H. Huang, Y. Wu, H. Feick, N. Tran, E. Weber and P. D. Yang, *Adv. Mater.*, 2001, **13**, 113.
22 J. Z. Wang, G. T. Du, Y. T. Zhang, B. J. Zhao, X. T. Yang and D. L. Liu, *J. Cryst. Growth*, 2004, **263**, 269.
23 A. B. Djurisic, W. C. H. Choy, V. A. L. Roy, Y. H. Leung, C. Y. Kwong, K. W. Cheah, T. K. G. Rao, W. K. Chan, H. T. Lui and C. Surya, *Adv. Funct. Mater.*, 2004, **14**, 856.